HHS Public Access

Author manuscript

DNA Repair (Amst). Author manuscript; available in PMC 2021 February 01.

Published in final edited form as:

DNA Repair (Amst). 2020 February ; 86: 102754. doi:10.1016/j.dnarep.2019.102754.

Loss of *Setd4* delays radiation-induced thymic lymphoma in mice

Xing Feng[a], **Huimei Lu**[a], **Jingyin Yue**[a], **Neta Schneider**[a], **Jingmei Liu**[a], **Lisa K Denzin**[b], **Chang S. Chan**[c], **Subhajyoti De**[c], **Zhiyuan Shen**[a,*]

[a]Rutgers Cancer Institute of New Jersey, Department of Radiation Oncology, Rutgers Robert Wood Johnson Medical School, 195 Little Albany Street, New Brunswick, New Jersey 08903, USA

[b]Child Health Institute of New Jersey, Rutgers Robert Wood Johnson Medical School, Rutgers University, New Brunswick, New Jersey, USA

[c]Center for Systems and Computational Biology, Rutgers Cancer Institute of New Jersey, Rutgers the State University of New Jersey. New Brunswick, NJ 08901, USA

Abstract

Radiation-induced lymphomagenesis results from a clonogenic lymphoid cell proliferation due to genetic alterations and immunological dysregulation. Mouse models had been successfully used to identify risk and protective factors for radiation-induced DNA damage and carcinogenesis. The mammalian SETD4 is a poorly understood putative methyltransferase. Here, we report that conditional *Setd4* deletion in adult mice significantly extended the survival of radiation-induced T-lymphoma. However, in Tp53 deficient mice, *Setd4* deletion did not delay the radiation-induced lymphomagenesis although it accelerated the spontaneous T-lymphomagenesis in non-irradiated mice. The T-lymphomas were largely clonogenic in both $Setd4^{flox/flox}$ and $Setd4^{\Delta/\Delta}$ mice based on sequencing analysis of the T-cell antigen β receptors. However, the $Setd4^{\Delta/\Delta}$ T-lymphomas were $CD4^{+}/CD8^{+}$ double positive, while the littermate $Setd4^{flox/flox}$ tumor were largely CD8+ single positive. A genomic sequencing analysis on chromosome deletion, inversion, duplication, and translocation, revealed a larger contribution of inversion but a less contribution of deletion to the overall chromosome rearrangements in the in $Setd4^{\Delta/\Delta}$ tumors than the $Setd4^{flox/flox}$ tumors. In addition, the $Setd4^{flox/flox}$ mice died more often from the large sizes of primary thymus lymphoma at earlier time, but there was a slight increase of lymphoma dissemination among peripheral

*To whom correspondence should be addressed at shenzh@cinj.rutgers.edu.

Authorship Contributions

XF and ZS: designed the experiments, performed data analysis, and drafted the initial version of manuscript. XF: performed most of the experiments; HL, JY, JL, and NS: performed and assisted some of the experiments. LD, CC, and SD: provided resources for flowcytometry and computational analyses and edited the manuscript. ZS: directed and oversaw the project, secured funding for the study, completed the final version of the manuscript.

Competing Interests

The authors declare that there were no competing interests.

organs in *Setd4*$^{\Delta/\Delta}$ at later times. These results suggest that *Setd4* has a critical role in modulating lymphomagenesis and may be targeted to suppress radiation-induced carcinogenesis.

Keywords

Setd4; T-cell lymphoma; radiation carcinogenesis; chromosome rearrangement; genomic instability

1. Introduction

Ionizing radiation (IR) is a potent DNA damage agent and a complete carcinogen, and can both initiate and promote tumorigenesis, largely due to oncogenic mutations resulting from DNA damage [1, 2]. The induction of T-lymphoma in mice upon fractionated irradiation has been proven to be a reliable approach to identify risk factors and protective modalities of radiation induced carcinogenesis [3-5]. Lymphomagenesis is characterized by the clonogenic proliferation of B, T or natural killer lymphoid cells[6-9]. Although the different types of lymphomas may have distinct cell lineage features, lymphomas may originate from the hematopoietic stem cells or uncommitted hematopoietic progenitor cells that evolved into tumor cells of distinct lineage features[10]. Lymphomagenesis is driven by DNA damage, genetic mutations, and immune dysregulation[11-13]. The use of genetically engineered mouse models have not only discovered the identifies of genes that contribute to human radiation carcinogenesis but also are valuable to complement human studies [3, 10]. Despite the successful identification of many genetic factors that initiate and propagate lymphomagenesis, additional genes that govern this process are yet to be discovered.

The mammalian SET domain-containing protein 4 (SETD4) is a putative methyltransferase of the SETD6 subfamily[14]. Members of this subfamily (SETD6, SETD3, and SETD4) share only ~20% amino acid identity with each other, yet they share a conserved substrate-binding domain similar with the plant Rubisco methyltransferase. Additionally, their SET domains are divided by an iSET region (insert of SET)[15-20]. SETD6 has been shown to methylate non-histone proteins, including p65/RelA of the NF-kB family, Polo-like kinase 1, PAK4 of the Wnt/beta-catenin pathway as well as other proteins[17, 21-24]. SETD3 was initially reported to methylate histones[25, 26], and two independent groups recently found that it can physiologically methylates a histidine residue in β-actin[18, 19, 27]. However, little is known about physiological substrates of the vertebrate and mammalian SETD4 *in vivo*, although the brine shrimp *Artemia Parthenogenetica* SETD4 can methylate histone H4K20 and H3K79[28].

Some correlative studies have implicated SETD4 in tumorigenesis and in the tumor response to treatment, including human ER-negative breast cancer[29], hepatocellular carcinoma sensitivity to sorafenib[30], and apoptosis in prostate cancer cells[31]. Oncogenic fusions of *SETD4* with FTCD, KIAA1958 and B4Galt6 have been observed in human cancers[32]. In the current study, we asked if Setd4 modulates radiation-induced cancer risk.

We found that *Setd4* deletion in adult mice extended the survival after radiation induced T-lymphomas. We further show that *Setd4* deficient T-lymphomas had distinct characteristics

compared to tumors that developed in wild type mice. These results suggested that SETD4 may be an attractive target to reduce the risk of radiation-induced lymphoma.

2. Materials and Methods

2.1. Mouse lines

The animal works presented in this study were approved by the Institutional Animal Care and Use Committee at Rutgers Robert Johnson Medical School. We adhered to and followed our institutional guideline regarding to animal welfare issues. Three mouse lines were used in this study.

Conditional Setd4 knockout mice: the construction and verification of conditional Setd4 ES clones and exon-6 deletion are detailed in Supplement Fig. S1 and S2. The PCR primer sequences for *Setd4* genotyping are summarized in Supplement Tables S1-S3, and the PCR primer locations are illustrated in Fig. 1A. DNA extracted from tail biopsy was used for PCR genotyping. A three-primer mix containing 5'-TCCTGGGCTCTGCCATCCATG, 5'-CTGTTGCAATGGAAATGCCAG, and 5'-CTAAAGCTCTGCCCTAAGGTC was used in multiplex PCR to identify the 234-bp wild type, 318-bp floxed, and 369-bp ΔExon6 *Setd4* alleles.

The Rosa26-CreERT2 mice (B6.129): obtained from Jackson Laboratory (Stock No 008463) and expressed CreERT2 under the control of a promoter at the endogenous Rosa26 locus. Administration of tamoxifen (Tam) can induce the translocation of the CreERT2 from cytoplasm to the nucleus, causing LoxP recombination. We crossed $Setd4^{flox/flox}$ mice with *Rosa26-CreERT2* to obtain $Setd4^{flox/flox}$;$Rosa26\text{-}CreERT2^{+}$ and $Setd4^{flox/wt}$;$Rosa26\text{-}CreERT2^{+}$ mice.

The $Tp53^{flox/flox}$ mice (B6.129): obtained from Jackson Laboratory (Stock No 008462) and carry a homozygous floxed exons 2-10 of the *Tp53* gene [33], and were crossed with $Setd4^{flox/flox}$;$Rosa26\text{-}CreERT2^{+/+}$ to generate $Setd4^{flox/flox}$;$Tp53^{flox/wt}$;$Rosa26\text{-}CreERT2^{+/+}$ and $Setd4^{flox/flox}$;$Tp53^{flox/flox}$;$Rosa26\text{-}CreERT2^{+/+}$. The primer-pair of 5′-GGTTAAACCCAGCTTGACCA and 5′-GGAGGCAGAGACAGTTGGAG was used to identify the 390-bp $Trp53^{floxExon2–10}$ and the 270-bp $Trp53^{wt}$ alleles. The primer-pair of 5′-GGTTAAACCCAGCTTGACCA and 5′-GAAGACAGAAAAGGGGAGGG was used to identify a 612-bp product of the LoxP-recombined $Tp53^{\Delta Exon2–10}$ allele.

2.2. Tam treatment and total body irradiation (TBI)

Tamoxifen (Sigma-Aldrich, T5648) was dissolved at a concentration of 25 mg/ml, in a mixture of 98% corn oil (Santa Cruz, sc-214761A) and 2% ethanol. A total of 160 μl per 25 g of body weight was injected intraperitoneally into 6-8 weeks old mice once per day for 5 days. Corn oil was used as the control. Five days after injections, mice were retained in a Rodent RadDisk and exposed to TBI using the Gammacell 40 Extractor (MDS Nordion) γ-irradiator at a dose rate of 91.6 cGy/min. The exact radiation doses will be given when describing the specific experiments.

2.3. Flow cytometric analysis

Single-cell suspensions were prepared from thymic lymphomas, spleen and lymph nodes, and stained with fluorochrome-conjugated antibodies: CD4 (APC-Cy7, L3T4, 47-0042-82, eBiosciences), CD8 (PerCP-Cy5.5, 53-6.7, 45-0081-82, eBiosciences), CD11b (A700, M1/70, 557960, BD Pharmingen), Gr-1 (FITC, RB6-8C5, 553127, BD Pharmingen). Data were acquired with an LSR II cytometer (BD Biosciences) using FACSDiva software and analyzed with FlowJo version 10 software (Tree Star). Cell doublets were excluded from all analyses and, when possible, dead cells were excluded by the use of DAPI. Collection media was RPMI1640 with 10% FBS, 1% Glutamine, 1% Penicillin/Streptomycin, 0.01% 2-Mercaptoethanol. FACS buffer is PBS supplemented with 1% FBS.

2.4. Histological and immunohistochemical (IHC) analyses

Tissue specimens were removed surgically, washed in cold PBS, fixed overnight in 10% formalin at 4°C, and transferred to 70% ethanol before submitting to institutional Biospecimen Repository and Histopathology Service for tissue processing. Paraffin-embedded tissue sections were cut at 5 μm and stained with hematoxylin and eosin (H&E). The procedure of an antigen retrieval and IHC staining was previously described [34, 35]. Briefly, antigen as retrieved with 0.05% citraconic anhydride (pH 7.4) by steaming the immersed slides in a kitchen steam cooker for 40 min after the temperature of the buffer reached 98°C. After retrieval, slides were washed in PBS and permeabilized with 0.1% Triton X-100 in PBS for 10 min followed by quenching of endogenous peroxides with 3% hydrogen peroxide for 15 min. BSA (3%) in PBS was used for blocking and dilution of antibodies. Immunoreactivity was visualized with 3,3′-diaminobenzidine (D5637; Sigma). Positive staining was visualized as a brown color precipitate that can be distinguished from the hematoxylin counterstain seen as a blue color. For immunofluorescent IHC, primary antibodies were incubated for 1 h at room temperature and washed three times for 5 min each in PBST. Goat anti-rat IgG secondary antibody, Alexa Fluor 488 (Thermo Fisher Scientific) or Rhodamine (TRITC) affinipure donkey anti-rabbit IgG (Jackson ImmunoResearch laboratories, Inc) was added to cover tissue area on the slides. Slides were incubated for 30 min at room temperature and washed three times for 5 min each in PBST. Commercial antibodies are: CD3 (A0452, Dako), B220/CD45R (103201, Biolegend), Ki67 (MA5-14520, Thermofisher Scientific), Cleaved caspase 3 (9661S, Cell Signaling Technology), CD4 (14-0041-81, Thermofisher Scientific), CD8 (361003, Synaptic Systems).

To semi-quantitatively assess lymphoma infiltration in peripheral organs, tissue sections of spleens, livers, kidneys, and lungs were stained for CD3 by IHC. Images were taken under microscope and CD3 positive cells were counted. Based on the percentage of CD3 positive cells, a semi-quantitative infiltration score was defined as: 0 (<5%), 1 (5-30%), 2 (30-60%), and 3 (>60%).

2.5. Tumor genomic sequencing

DNA were subjected to genomic sequencing by GENEWIZ with paired end reads. We mapped the reads from the low pass whole genome sequencing experiments to the mouse reference genome GRCm38 using BWA[36] after an initial quality control check using FastQC (http://www.bioinformatics.babraham.ac.uk/projects/fastqc). The genome-wide

depth of read coverage was ~1X. This appeared to have low technical variations between samples, between chromosomes within the same sample, and between adjacent regions within the same chromosome, apart from the cases where copy number alterations resulted in systematic, sharp transition in depth of coverage. We used Delly2[37], with default parameter settings, to identify structural variations (SV) including genomic junction-points in the samples. We compared the catalog of SV calls in each tumor sample against pooled SV calls from the normal tissue samples and excluded those that have junction-points within 1 kb of SV junction-points in normal tissues to call somatic SVs in the tumor samples. This approach enabled us to avoid spuriously overcalling somatic SVs in the tumors due to imprecise junction-point identification and/or low regional coverage in any individual normal control sample. The SVs were classified into four categories (DEL: deletions, DUP: duplications, INV: inversions, and TRA: inter-chromosomal translocations), based on genomic mapping and clustering of the split reads and paired end reads as shown before[37]. If the SV junction had sufficient split read support, the junction sequence and precise DNA junction-point can be ascertained. But when there is no split read support, or there is extended homology at the junction (e.g. longer than the read length) the junction sequence and DNA junction-point cannot be determined precisely. We anticipate that most of the SVs would be called at ~1X coverage, but due to modest depth of coverage, a majority (>90%) of the reported SVs had imprecise junction-points. For the SVs with precise junction-points, the length of homology between the adjoining genomic regions enabled us to infer the likely mechanism of DNA end rejoining. We classified the SVs with homology length of 0-3 bp, 4-9 bp, and >9 bp at the junction-points to have limited, medium, and extended homology. In general, SVs with limited and extended homology are suspected to arise due to NHEJ and HR-mediated repair respectively[38].

2.6. Sequencing of T-cell receptor β (TCRβ)

DNA was extracted from 30 mg of thymic lymphoma tissue using the MagAttract HMW DNA Kit (Qiagen, 67563), and submitted to Adaptive Biotechologies to sequence the TCRβ using the ImmunoSeq survey assay, and the data were analyzed using the ImmunoSeq Analyzer (Adaptive Biotechnologies) to determine the clonogenicity of the tumor DNA as well as the nature of the V(D)J rearrangement and whether it leads to a productive template for functional TCRβ.

2.7. Statistics

Statistical analysis was performed using Prism Software (GraphPad). Statistical differences were determined with the Student's *t*-test and Log-rank (Mantel-Cox) test. Unless the P-value is specifically shown, statistical significance was defined as $*P < 0.05$, $**P < 0.01$, and $***P < 0.001$.

3. Results

3.1. Generation of Tam-inducible adult Setd4 knockout mice

To investigate the biological functions of SETD4 *in vivo*, we converted a trapped *Setd4* allele in an ES clone to an allele with *Setd4* exon 6 floxed (see Fig. S1). The new ES clone was then used to generate founder $Setd4^{flox/wt}$ mice, and subsequently $Setd4^{flox/flox}$ mice.

After the expected deletion of exon 6 upon Cre-expression in the *Setd4*$^{flox/flox}$ mouse embryo fibroblasts (MEF) was verified on genomic DNA and mRNA levels (Fig. S2), the *Setd4*$^{flox/flox}$ mice were mated with the *Rosa26-CreERT2* mice[39], to generate *Setd4*$^{flox/flox}$;*Rosa26-CreERT2*$^{+}$. Six- to eight-week old adult mice were administrated with Tam to induce deletion of exon 6 in *Setd4*. As shown in Fig. 1A, 1B, there was a successful deletion of *Setd4* exon 6 among the majorities of the tissues, except brain. In agreement, there were consequential down-regulations of *Setd4* mRNA in these tissues (Fig. 1C). Therefore, an inducible conditional *Setd4* knockout mouse model was established. Notably, Tam-treated adult *Setd4*$^{flox/flox}$;*Rosa26-CreERT2*$^{+}$ (*Setd4*$^{\Delta/\Delta}$) mice were viable and didn't display any obvious growth retardation or a tendency of tumor development compared to Oil-treated mice (Fig. 1D).

3.2. Loss of Setd4 extends the survival of radiation-induced thymic lymphoma

To address if loss of *Setd4* impacted the risk of radiation-induced carcinogenesis, we induced *Setd4* deletion in adult *Setd4*$^{flox/flox}$;*Rosa26-CreERT2*$^{+}$ mice by Tam injection, resulting *Setd4*$^{\Delta/\Delta}$ mice. Sex-matched littermates injected with vehicle (oil) were used as controls (*Setd4*$^{flox/flox}$). We irradiated (or sham-irradiated as controls) groups of mice with 2 Gy of gamma-rays weekly for 4 weeks (4 × 2Gy). As predicted, these mice developed lymphomas, mainly in thymus. In some mice, tumor cell infiltrations were observed in the spleen, liver, kidney, lung, and other organs (Fig. 2A, S3). The lymphoma cells were positive for Ki-67 and the T-cell marker CD3 but negative of the B-cell marker B220/CD45R (Fig. 2B, S3), suggesting that the tumors were T-cell lymphoma.

During the initial 100 to 300 days after irradiation, all died mice had thymic lymphomas. Intriguingly, the loss of *Setd4* significantly delayed the death of radiation-induced thymic lymphoma and improved the overall survival (Fig. 2C). The median survival was 195 days for *Setd4*$^{flox/flox}$ mice, but 245 days for *Setd4*$^{\Delta/\Delta}$ mice. At the end of the experiment (500 days after irradiation), the lymphoma-free survival for *Setd4*$^{\Delta/\Delta}$ mice was 22% (11 out of 50), but 9.4% (5 out of 53) for the *Setd4*$^{flox/flox}$ (Fig. 2C, P=0.078 by Chi-Square test). Tam-treatment of wild type mice (*Setd4*$^{wt/wt}$;*Rosa26-CreERT2*$^{+}$) did not alter the time course of radiation induced tumor development from Oil treated littermates (Fig. S4). Genotyping of tumor DNA confirmed the *Setd4* deletion in the lymphomas and tumor infiltrated organs of the *Setd4*$^{\Delta/\Delta}$ mice (Fig. 3D). Collectively, these data show that loss of *Setd4* significantly delayed the development of radiation-induced thymic lymphoma and the lymphoma-mediated death.

Next, we compared the general features of the lymphomas that developed in the *Setd4*$^{flox/flox}$ and *Setd4*$^{\Delta/\Delta}$ mice. As shown in Fig. 3A, there was little significant difference of primary thymus tumor size at the time of death, although there was a slight decrease of tumor sizes among the *Setd4*$^{\Delta/\Delta}$ animals that died within the first 195 days, which is the median survival for the *Setd4*$^{flox/flox}$ mice. The quicker growing tumors likely contributes to the earlier death of the *Setd4*$^{flox/flox}$ mice. We also observed a higher percentage of cleaved caspase-3 positive cells in the tumors from *Setd4*$^{flox/flox}$ mice than from *Setd4*$^{\Delta/\Delta}$ (Fig. 3B). An increased apoptotic feature had been suggested to associate with a higher grade of malignancy[40]. Although both mice have T-lymphoma cells that have disseminated to

peripheral organs, *Setd4*$^{\Delta/\Delta}$ mice have a more widespread peripheral organs infiltration by the T-lymphoma cells, especially to the spleen, liver, kidney, and lung (Fig. 3C). Based on the percentage of tumor cells in the four main organs (Table 1), we calculated a semi-quantitative Tumor Dissemination Score (see Materials and Methods) Although the *Setd4*$^{\Delta/\Delta}$ died later than the *Setd4*$^{flox/flox}$, they generally had higher tumor dissemination score at the time of death (Fig. 3D). Overall, these data demonstrate that *Setd4*$^{\Delta/\Delta}$ mice died later than *Setd4*$^{flox/flox}$ likely due to slower tumor enlargement in the thymuses, and the loss of *Setd4* promoted the dissemination of T lymphoma cells at later time points.

3.3 Cellular subtypes of thymic lymphoma in Setd4$^{\Delta/\Delta}$ mice

We next determined the subtypes of thymic lymphomas that developed in the two strains of mice. Single cell suspensions from available thymic lymphomas were stained with fluorphone conjugated antibodies specific for CD4 and CD8 followed by flow cytometry to determine the T cell subsets populating the T lymphomas. As shown in Fig. 4A, the *Setd4*$^{flox/flox}$ thymic tumors were composed of T cells mainly expressing only positive CD8, which is in agreement with what has been previously reported [41, 42]. However, the *Setd4*$^{\Delta/\Delta}$ thymic lymphomas were mainly composed of T cells expressing both CD8 and CD4 (Fig. 4A). In spleens that had been infiltrated with tumor cells, there were also higher percentages of CD8 and CD4 double positive cells in *Setd4*$^{\Delta/\Delta}$ mice than in *Setd4*$^{flox/flox}$ mice (Fig. 4B). To confirm these findings, IHC and immunofluorescene were used to analyze thymic tumors from 14 *Setd4*$^{flox/flox}$ and 11 *Setd4*$^{\Delta/\Delta}$ mice (Fig. 4C and 4D). These studies confirmed that found all tumors were CD8 positive, but many (9 out of 11) of the *Setd4*$^{\Delta/\Delta}$ tumors were also 100% CD4 positive (i.e. CD4 and CD8 double positive), while fewer of the *Setd4*$^{flox/flox}$ tumors (5 out of 14) were 100% CD4 positive. These differences were found to be statistically significant (Chi-Square test, $p = 0.016$) (Fig. 4E). Together these data show *Setd4* loss altered the subtype of T cells comprise the thymic tumors. *Setd4*$^{\Delta/\Delta}$ tumors were composed mainly composed of CD8/CD8 double positive cells whereas tumors in *Setd4*$^{flox/flox}$ mice are mainly CD8 single positive.

3.3. Genomic rearrangements and clonality in radiation-induced lymphomas

It is known that radiation induced DNA double strand break is the major cause of genomic instability that lead to the development of T-lymphoma. To investigate whether *Setd4* affected the types of chromosome rearrangements found in tumor, we performed genome sequencing analysis (see Materials and Methods). Based on the analysis of tumor DNA from *Setd4*$^{\Delta/\Delta}$ (N=9) and *Setd4*$^{flox/flox}$ (N=7) mice, we found that in *Setd4*$^{\Delta/\Delta}$ thymic lymphomas, the contribution of DNA deletion was significantly less than in *Setd4*$^{flox/flox}$. However, there was a significantly increased contribution of chromosome inversion (Fig. 5A). This data further demonstrates that the *Setd4* deficiency not only altered overall tumor risk, the kinetics of lymphoma development and composition of the of the radiation induced T lymphomas (Fig. 2, 4), but also altered the fundamental process of tumor development.

We also determined if the tumors were derived from a single cell or were due to polyclonal expansion many cells. To determine clonality of the thymic lymphomas, we sequenced the T-cell antigen receptor β (TCRβ) locus for 7 *Setd4*$^{flox/flox}$ tumors (4 male and 3 females) and 7 *Setd4*$^{\Delta/\Delta}$ tumors (4 males and 3 females), using a previously described approach[42,

43]. We found that the relative contribution of productive vs. non-productive V(D)J rearrangements was not significantly different between *Setd4*$^{flox/flox}$ and *Setd4*$^{\Delta/\Delta}$ tumors, and almost all tumors had a single dominant clone that had a productive V(D)J rearrangement (Fig. 5B). Furthermore, most of the radiation-induced lymphomas were derived from the expansion of a single dominant clone independent the Setd4 status (Fig. 5C). These data suggested that *Setd4* loss does not impact clonal expansion of T-lymphoma development after irradiation, thus unlikely to directly impact on the V(D)J process or the negative selection of non-productive rearrangements leading to nonfunctional TCRβ in the thymic lymphomas.

3.4. Modulation of Tp53 deficiency induced T-lymphomagenesis by Setd4

Loss of *Tp53* not only increases the risk of spontaneous T-lymphoma, but also markedly accelerates radiation-induced thymic lymphoma[5]. Because loss of *Setd4* extends the survival of radiation-induced thymic lymphoma, we determined whether *Setd4* loss would also delay the tumor development in *Tp53* deficient mice. We used the Tam-inducible knockout approach with *Tp53*$^{flox/flox}$*;Rosa26-CreERT2* mice[33]. The structure of the Tp53 allele and PCR genotyping strategy used are illustrated in Fig. S5A, S5B. The effectiveness of Tam-induced Tp53 deletion was confirmed by PCR and western blots (Fig. S5C, S5D). *Setd4*$^{flox/flox}$*;Rosa26-CreERT2*$^{+}$ mice were crossed with *Tp53*$^{flox/flox}$, to allow for *Setd4* and *Tp53* double deletion after tamoxifen treatment. First, we observed that spontaneous tumorigenesis in the *Tp53* deficient mouse cohorts, including the time course of the tumor formation and tumor types (Fig. S6) were similar to previously reported by others [44, 45]. Co-deletion of *Setd4* significantly accelerated spontaneous tumor development in *Tp53*$^{\Delta/\Delta}$ (P=0.0129) but not in *Tp53*$^{\Delta/wt}$ mice (p=0.0796) (Fig. 6A).

We next investigated whether *Setd4* deletion altered radiation-induced lymphoma development in *Tp53* deficient mice using the same 4×2Gy radiation exposure scheme as in Fig. 2C. We found that exposure to radiation accelerated thymic lymphoma formation in the *Tp53*$^{\Delta/\Delta}$ mice and majority of these tumors caused death within 100 days post TBI (compare Fig. 6B with 6A). This radiation accelerated thymic tumor formation was also observed in the *Tp53*$^{\Delta/wt}$ mice (compare Fig. 6C with 6A). However, co-deletion of *Setd4* in these mice did not affect the tumor development in *Setd4*$^{\Delta/\Delta}$*;Tp53*$^{\Delta/\Delta}$ mice (Fig. 6B) or *Setd4*$^{\Delta/\Delta}$*;Tp53*$^{\Delta/wt}$ (Fig. 6C) as in the case of p53 wild type mice (Fig. 2C). Furthermore, *Setd4*$^{\Delta/\Delta}$*;Tp53*$^{\Delta/\Delta}$ mice mainly died of non-disseminated thymic lymphomas (tumors confined to the thymus), unlike *Setd4*$^{\Delta/\Delta}$ mice in which the tumors were widely disseminated to other organs. The *Setd4*$^{\Delta/\Delta}$*;Tp53*$^{\Delta/\Delta}$ thymic lymphoma were significantly larger in size (Fig. 6D). Thus, loss of *Setd4* failed to delay radiation-induced thymic lymphoma in a *Tp53* deficient background. In other words, p53 deficiency overrode the effect of *Setd4* deficiency induced delay of radiation carcinogenesis. However, *Setd4* deletion can accelerate the development of spontaneous lymphoma in p53 null mice (Fig. 6A).

4. Discussion

In this report, we showed that the induced deletion of mouse *Setd4* in adults extended the mouse survival in a radiation-induced T cell lymphoma model. *Setd4* deficient T-lymphomas were composed of mostly CD4/CD8 double positive T lymphoma cells and had unique genomic rearrangement patterns that were distinct from wild type tumors, but yet, like wild tumors, were derived from single clonotypes.

Radiation damage induced lymphomagenesis often begins prior to T cell development in the thymus and is thought begin in the hematopoietic stem/progenitor cells in the bone marrow[2], since it can be prevented by shielding part of bones or transplanting healthy hematopoietic stem/progenitor cells[46, 47]. The induction of mouse T-lymphoma by fractionated γ-radiation exposure is a classical model to study radiation carcinogenesis. Using this experimental model, both risk factors, such as p53 deletion[5], and protective modalities, such as deletions of TLR4[48], have been successfully identified for T-lymphoma development. Our study established *Setd4* as a previously unknown modulator of radiation induced lymphomagenesis. The extended T-lymphoma survival of the *Setd4* deficient mice indicated that *Setd4* itself may have an oncogenic activity. This is in agreement with the recent identifications of *SETD4* oncogenic fusions (see supplement Table in Gao et al[32]), and the correlative *SETD4* expression in cancers [29-31].

It is likely that the effects of *Setd4* deletion on the survival from T-lymphoma could be attributed by either the intrinsic property of the *Setd4* deficient tumor cells, and/or the *Setd4* depleted tumor environment in the mice. Two lines of evidence suggested that *Setd4* deletion affected the intrinsic properties of the tumor cells. First, the *Setd4* deficient T-lymphoma were mostly CD4/CD8 double positive, while the tumors developed in wild type mice were mostly CD8 single positive. Second, genome sequencing revealed that there were more inversions events but fewer deletion events in the $Setd4^{\Delta/\Delta}$ tumor than the $Setd4^{flox/flox}$ tumors (Fig. 5A). Although the $Setd4^{\Delta/\Delta}$ tumors had were more likely to disseminate to other tissues than the wild type tumors (Fig. 3), the $Setd4^{\Delta/\Delta}$ tumors were analyzed at a slightly later time frame due to delayed death of $Setd4^{\Delta/\Delta}$ mice. Thus, a full understanding of *Setd4* function in mediating tumor dissemination and the contribution of the tumor environment will require future investigation.

In our studies, Setd4 deletion was induced in adult mice. Thus, our mouse model avoided potential adverse effects of development due to Setd4 deletion during embryogenesis and at young ages, which can be unavoidable when constitutive Setd4 knockout is used. During T cell development in the thymus, the developing T cells transition through a CD4/CD8 double positive stage[49] followed by further differentiated into CD4 or CD8 single positive cells. Our discovery that the T lymphomas from $Setd4^{\Delta/\Delta}$ mice were mostly CD4/CD8 double positive suggests that tumors in these mice are derived from less differentiated cells compared to T lymphomas from $Setd4^{flox/flox}$ mice which are mostly CD8 single positive. Differential development of normal CD4 and CD8 double positive cells have been linked to numerous diseases including cancer[49]. The majority of T cell development takes place in young mice. An analysis of T cell population in the normal spleens did not show any difference of the relative abundance of the CD4 and CD8 cells (data not shown).

The immunological tumor microenvironment is a known determinant for tumor infiltration through the regulation of pro-tumor cytokines[50]. Myeloid-derived suppressor cell (MDSCs) are a heterogeneous population of suppressive innate immune cells that exists only in pathological conditions such as chronic inflammation and cancer [51, 52]. MDSCs suppress both innate and adaptive immunity within tumor microenvironments via the production of immune-suppressive molecules [51]. The presence of MDSC in the tumor tissue is considered an indicator of an immunologically suppressed microenvironment [53] and is strongly associated with metastasis [54]. Therefore, we measured MDSCs (phenotypically defined as defined as $CD11b^{+}$, $Gr\text{-}1^{+}$) in tumors from *Setd4* deficient mice that had infiltrated peripheral tissues. However, we did not observe any significant differences in the percentage of MDSCs in $Setd4^{\Delta/\Delta}$ and $Setd4^{flox/flox}$ mice (Fig. S7). Toll-like receptor 4 (TLR-4) deficient mice show delayed tumorigenesis after irradiation[48]. We noticed that the delayed T-lymphoma development (Fig. 2C) was very much like a phenocopy of the TLR4 deficient mice [48] after radiation. While this manuscript was in the final preparation, a new report suggested that constitutive Setd4 deletion can abrogate TLR agonist LPS elicited cytokine-induction in macrophages [55]. Thus, it is possible that Setd4 is a down-stream mediator of the TLR elicited tumor progression that may contribute to the tumor-environment interaction, a hypothesis to be tested in the future. It had been suggested that H4K20 and H3K79 might be the substrates of human and *Artemia* SETD4[28, 56]. However, a recent report was not able to confirm these sites, and it instead suggested H3K4 as a substrate of SETD4 in macrophages [55]. Thus, an important question to be addressed in the future is the identities of the physiological substrate(s) of SETD4 in the context of radiation-induced carcinogenesis.

In summary, our studies show that *Setd4* deficiency delays radiation-induced development of T-lymphoma in adult mice, and that these lymphomas were mostly CD4/CD8 double positive. These findings may have important implications to reduce cancer risk caused by radiation-induced DNA damage.

Supplementary Material

Refer to Web version on PubMed Central for supplementary material.

Acknowledgments

This research was supported by NIH R01CA156706 and R01CA195612 grants to ZS, by support from Robert Wood Johnson Foundation to CINJ, and by the Biospecimen Repository and Histopathology Service, Genome Editing, of The Rutgers Cancer Institute of New Jersey (P30CA072720). The authors thank Drs. Ping Xie, Sam Bunting (Rutgers, the State University of New Jersey) for suggestions throughout the study.

References

[1]. Little JB, Radiation carcinogenesis, Carcinogenesis, 21 (2000) 397–404. [PubMed: 10688860]

[2]. KAPLAN HS, The role of radiation in experimental leukemogenesis, Natl Cancer Inst Monogr, 14 (1964) 207–217. [PubMed: 14147133]

[3]. Seto M, Molecular mechanisms of lymphomagenesis through transcriptional disregulation by chromosome translocation, International journal of hematology, 76 (2002) 323–326. [PubMed: 12430874]

[4]. Labi V, Erlacher M, Kiessling S, Manzl C, Frenzel A, O'Reilly L, Strasser A, Villunger A, Loss of the BH3-only protein Bmf impairs B cell homeostasis and accelerates γ irradiation–induced thymic lymphoma development, Journal of Experimental Medicine, 205 (2008) 641–655. [PubMed: 18299399]

[5]. Kemp CJ, Wheldon T, Balmain A, p53-deficient mice are extremely susceptible to radiation-induced tumorigenesis, Nature genetics, 8 (1994) 66. [PubMed: 7987394]

[6]. Jaffe ES, Harris NL, Stein H, Isaacson PG, Classification of lymphoid neoplasms: the microscope as a tool for disease discovery, Blood, 112 (2008) 4384–4399. [PubMed: 19029456]

[7]. Sahasrabuddhe AA, Elenitoba-Johnson KS, The role of aberrant proteolysis in lymphomagenesis, Current opinion in hematology, 22 (2015) 369. [PubMed: 26049759]

[8]. ES J, NL H, JW SH,V, Pathology and genetics of tumours of haematopoietic and lymphoid tissues. , IARC Press, Lyon, France, 2001.

[9]. Goldin LR, Landgren O, Autoimmunity and lymphomagenesis, International journal of cancer, 124 (2009) 1497–1502. [PubMed: 19089924]

[10]. Weigert O, Weinstock DM, The evolving contribution of hematopoietic progenitor cells to lymphomagenesis, Blood, 120 (2012) 2553–2561. [PubMed: 22869790]

[11]. Kušec R, Molecular and genetic mechanisms of lymphomagenesis, Croat Med J, 43 (2002) 519–525. [PubMed: 12402389]

[12]. Taylor JG, Gribben JG, Microenvironment abnormalities and lymphomagenesis: Immunological aspects, in: Seminars in cancer biology, Elsevier, 2015, pp. 36–45.

[13]. Puebla-Osorio N, Zhu C, DNA damage and repair during lymphoid development: antigen receptor diversity, genomic integrity and lymphomagenesis, Immunologic research, 41 (2008) 103–122. [PubMed: 18214391]

[14]. Petrossian TC, Clarke SG, Uncovering the human methyltransferasome, Molecular & Cellular Proteomics, 10 (2011) M110. 000976.

[15]. Trievel RC, Flynn EM, Houtz RL, Hurley JH, Mechanism of multiple lysine methylation by the SET domain enzyme Rubisco LSMT, Nature Structural Biology, 10 (2003) 545. [PubMed: 12819771]

[16]. Trievel RC, Beach BM, Dirk LMA, Houtz RL, Hurley JH, Structure and Catalytic Mechanism of a SET Domain Protein Methyltransferase, Cell, 111 (2002) 91–103. [PubMed: 12372303]

[17]. Chang Y, Levy D, Horton JR, Peng J, Zhang X, Gozani O, Cheng X, Structural basis of SETD6-mediated regulation of the NF-kB network via methyl-lysine signaling, Nucleic acids research, 39 (2011) 6380–6389. [PubMed: 21515635]

[18]. Wilkinson AW, Diep J, Dai S, Liu S, Ooi YS, Song D, Li TM, Horton JR, Zhang X, Liu C, Trivedi DV, Ruppel KM, Vilches-Moure JG, Casey KM, Mak J, Cowan T, Elias JE, Nagamine CM, Spudich JA, Cheng X, Carette JE, Gozani O, SETD3 is an actin histidine methyltransferase that prevents primary dystocia, Nature, 565 (2019) 372–376. [PubMed: 30626964]

[19]. Guo Q, Liao S, Kwiatkowski S, Tomaka W, Yu H, Wu G, Tu X, Min J, Drozak J, Xu C, Structural insights into SETD3-mediated histidine methylation on beta-actin, eLife, 8 (2019).

[20]. Abaev-Schneiderman E, Admoni-Elisha L, Levy D, SETD3 is a positive regulator of DNA-damage-induced apoptosis, Cell Death Dis, 10 (2019) 74. [PubMed: 30683849]

[21]. Levy D, Kuo AJ, Chang Y, Schaefer U, Kitson C, Cheung P, Espejo A, Zee BM, Liu CL, Tangsombatvisit S, Lysine methylation of the NF-κB subunit RelA by SETD6 couples activity of the histone methyltransferase GLP at chromatin to tonic repression of NF-κB signaling, Nature immunology, 12 (2011) 29. [PubMed: 21131967]

[22]. Vershinin Z, Feldman M, Chen A, Levy D, PAK4 Methylation by SETD6 Promotes the Activation of the Wnt/beta-Catenin Pathway, The Journal of biological chemistry, 291 (2016) 6786–6795. [PubMed: 26841865]

[23]. Levy D, Liu CL, Yang Z, Newman AM, Alizadeh AA, Utz PJ, Gozani O, A proteomic approach for the identification of novel lysine methyltransferase substrates, Epigenetics & chromatin, 4 (2011) 19. [PubMed: 22024134]

[24]. Feldman M, Vershinin Z, Goliand I, Elia N, Levy D, The methyltransferase SETD6 regulates Mitotic progression through PLK1 methylation, Proceedings of the National Academy of Sciences of the United States of America, 116 (2019) 1235–1240. [PubMed: 30622182]

[25]. Kim DW, Kim KB, Kim JY, Seo SB, Characterization of a novel histone H3K36 methyltransferase setd3 in zebrafish, Biosci Biotechnol Biochem, 75 (2011) 289–294. [PubMed: 21307598]

[26]. Eom GH, Kim KB, Kim JH, Kim JY, Kim JR, Kee HJ, Kim DW, Choe N, Park HJ, Son HJ, Choi SY, Kook H, Seo SB, Histone methyltransferase SETD3 regulates muscle differentiation, The Journal of biological chemistry, 286 (2011) 34733–34742. [PubMed: 21832073]

[27]. Kwiatkowski S, Seliga AK, Vertommen D, Terreri M, Ishikawa T, Grabowska I, Tiebe M, Teleman AA, Jagielski AK, Veiga-da-Cunha M, Drozak J, SETD3 protein is the actin-specific histidine N-methyltransferase, eLife, 7 (2018).

[28]. Dai L, Ye S, Li HW, Chen DF, Wang HL, Jia SN, Lin C, Yang JS, Yang F, Nagasawa H, Yang WJ, SETD4 Regulates Cell Quiescence and Catalyzes the Trimethylation of H4K20 during Diapause Formation in Artemia, Molecular and cellular biology, 37 (2017).

[29]. Faria JAQA, Corrêa NCR, de Andrade C, de Angelis Campos AC, dos R Santos Samuel de Almeida, T.S. Rodrigues, A.M. de Goes, D.A. Gomes, F.P. Silva, SET domain-containing Protein 4 (SETD4) is a Newly Identified Cytosolic and Nuclear Lysine Methyltransferase involved in Breast Cancer Cell Proliferation, Journal of cancer science & therapy, 5 (2013) 58–65. [PubMed: 24738023]

[30]. Li G-M, Wang Y-G, Pan Q, Wang J, Fan J-G, Sun C, RNAi screening with shRNAs against histone methylation-related genes reveals determinants of sorafenib sensitivity in hepatocellular carcinoma cells, International journal of clinical and experimental pathology, 7 (2014) 1085. [PubMed: 24696725]

[31]. Zhu S, Xu Y, Song M, Chen G, Wang H, Zhao Y, Wang Z, Li F, PRDM16 is associated with evasion of apoptosis by prostatic cancer cells according to RNA interference screening, Molecular medicine reports, 14 (2016) 3357–3361. [PubMed: 27511603]

[32]. Gao Q, Liang WW, Foltz SM, Mutharasu G, Jayasinghe RG, Cao S, Liao WW, Reynolds SM, Wyczalkowski MA, Yao L, Yu L, Sun SQ, Chen K, Lazar AJ, Fields RC, Wendl MC, Van Tine BA, Vij R, Chen F, Nykter M, Shmulevich I, Ding L, Driver Fusions and Their Implications in the Development and Treatment of Human Cancers, Cell reports, 23 (2018) 227–238.e223. [PubMed: 29617662]

[33]. Marino S, Vooijs M, van der Gulden H, Jonkers J, Berns A, Induction of medulloblastomas in p53-null mutant mice by somatic inactivation of Rb in the external granular layer cells of the cerebellum, Genes & development, 14 (2000) 994–1004. [PubMed: 10783170]

[34]. Huang YY, Dai L, Gaines D, Droz-Rosario R, Lu H, Liu J, Shen Z, BCCIP Suppresses Tumor Initiation but Is Required for Tumor Progression, Cancer research, 73 (2013) 7122–7133. [PubMed: 24145349]

[35]. Lu H, Huang YY, Mehrotra S, Droz-Rosario R, Liu J, Bhaumik M, White E, Shen Z, Essential roles of BCCIP in mouse embryonic development and structural stability of chromosomes, PLoS Genet, 7 (2011) e1002291. [PubMed: 21966279]

[36]. Robertson SA, Rae CJ, Graham A, Induction of angiogenesis by murine resistin: putative role of PI3-kinase and NO-dependent pathways, Regulatory peptides, 152 (2009) 41–47. [PubMed: 18722482]

[37]. Rausch T, Zichner T, Schlattl A, Stütz AM, Benes V, Korbel JO, DELLY: structural variant discovery by integrated paired-end and split-read analysis, Bioinformatics, 28 (2012) i333–i339. [PubMed: 22962449]

[38]. Yang L, Luquette LJ, Gehlenborg N, Xi R, Haseley PS, Hsieh C-H, Zhang C, Ren X, Protopopov A, Chin L, Diverse mechanisms of somatic structural variations in human cancer genomes, Cell, 153 (2013) 919–929. [PubMed: 23663786]

[39]. Hayashi S, McMahon AP, Efficient recombination in diverse tissues by a tamoxifen-inducible form of Cre: a tool for temporally regulated gene activation/inactivation in the mouse, Developmental biology, 244 (2002) 305–318. [PubMed: 11944939]

[40]. Soini Y, Pääkkö P, Lehto V, Histopathological evaluation of apoptosis in cancer, The American journal of pathology, 153 (1998) 1041–1053. [PubMed: 9777936]

[41]. Introcaso CE, Kim EJ, Gardner J, Junkins-Hopkins JM, Vittorio CC, Rook AH, CD8+ epidermotropic cytotoxic T-cell lymphoma with peripheral blood and central nervous system involvement, Archives of dermatology, 144 (2008) 1027–1029. [PubMed: 18711076]

[42]. Bachy E, Urb M, Chandra S, Robinot R, Bricard G, De Bernard S, Traverse-Glehen A, Gazzo S, Blond O, Khurana A, CD1d-restricted peripheral T cell lymphoma in mice and humans, Journal of Experimental Medicine, 213 (2016) 841–857. [PubMed: 27069116]

[43]. Dudgeon C, Chan C, Kang W, Sun Y, Emerson R, Robins H, Levine AJ, The evolution of thymic lymphomas in p53 knockout mice, Genes Dev, 28 (2014) 2613–2620. [PubMed: 25452272]

[44]. Donehower LA, Harvey M, Slagle BL, McArthur MJ, Montgomery CA Jr, Butel JS, Bradley A, Mice deficient for p53 are developmentally normal but susceptible to spontaneous tumours, Nature, 356 (1992) 215. [PubMed: 1552940]

[45]. Jacks T, Remington L, Williams BO, Schmitt EM, Halachmi S, Bronson RT, Weinberg RA, Tumor spectrum analysis in p53-mutant mice, Current biology, 4 (1994) 1–7. [PubMed: 7922305]

[46]. Kaplan HS, Brown MB, Paull J, Influence of bone-marrow injections on involution and neoplasia of mouse thymus after systemic irradiation, JNCI: Journal of the National Cancer Institute, 14 (1953) 303–316. [PubMed: 13097153]

[47]. Kaplan HS, Brown MB, Protection against radiation-induced lymphoma development by shielding and partial-body irradiation of mice, Cancer Research, 12 (1952) 441–444. [PubMed: 14936011]

[48]. Liu C, Gao F, Li B, Mitchel R, Liu X, Lin J, Zhao L, Cai J, TLR4 knockout protects mice from radiation-induced thymic lymphoma by downregulation of IL6 and miR-21, Leukemia, 25 (2011) 1516. [PubMed: 21617699]

[49]. Overgaard NH, Jung JW, Steptoe RJ, Wells JW, CD4+/CD8+ double- positive T cells: more than just a developmental stage?, Journal of leukocyte biology, 97 (2015) 31–38. [PubMed: 25360000]

[50]. Joyce JA, Fearon DT, T cell exclusion, immune privilege, and the tumor microenvironment, Science, 348 (2015) 74–80. [PubMed: 25838376]

[51]. Gabrilovich DI, Ostrand-Rosenberg S, Bronte V, Coordinated regulation of myeloid cells by tumours, Nature Reviews Immunology, 12 (2012) 253.

[52]. Youn J-I, Nagaraj S, Collazo M, Gabrilovich DI, Subsets of myeloid-derived suppressor cells in tumor-bearing mice, The Journal of Immunology, 181 (2008) 5791–5802. [PubMed: 18832739]

[53]. Kumar V, Patel S, Tcyganov E, Gabrilovich DI, The nature of myeloid-derived suppressor cells in the tumor microenvironment, Trends in immunology, 37 (2016) 208–220. [PubMed: 26858199]

[54]. Condamine T, Ramachandran I, Youn J-I, Gabrilovich DI, Regulation of tumor metastasis by myeloid-derived suppressor cells, Annual review of medicine, 66 (2015) 97–110.

[55]. Zhong Y, Ye P, Mei Z, Huang S, Huang M, Li Y, Niu S, Zhao S, Cai J, Wang J, Zou H, Jiang Y, Liu J, The novel methyltransferase SETD4 regulates TLR agonist-induced expression of cytokines through methylation of lysine 4 at histone 3 in macrophages, Molecular immunology, 114 (2019) 179–188. [PubMed: 31376731]

[56]. Ye S, Ding YF, Jia WH, Liu XL, Feng JY, Zhu Q, Cai SL, Yang YS, Lu QY, Huang XT, Yang JS, Jia SN, Ding GP, Wang YH, Zhou JJ, Chen YD, Yang WJ, SET Domain-Containing Protein 4 Epigenetically Controls Breast Cancer Stem Cell Quiescence, Cancer Res, 79 (2019) 4729–4743. [PubMed: 31308046]

Highlights:

- The *Setd4* gene plays a role in tumorigenesis.
- Induced *Setd4* deletion in adult mice delayed the development of radiation-induced T- lymphomas.
- The *Setd4* deficient T-lymphomas had distinct CD8/CD4 marker distribution.
- Setd4 deletion accelerated the spontaneous lymphoma development but did not alter the radiation induced T-lymphoma in Tp53 deficient mice.
- The study suggests Setd4 as a potential target to suppress lymphoma progression.

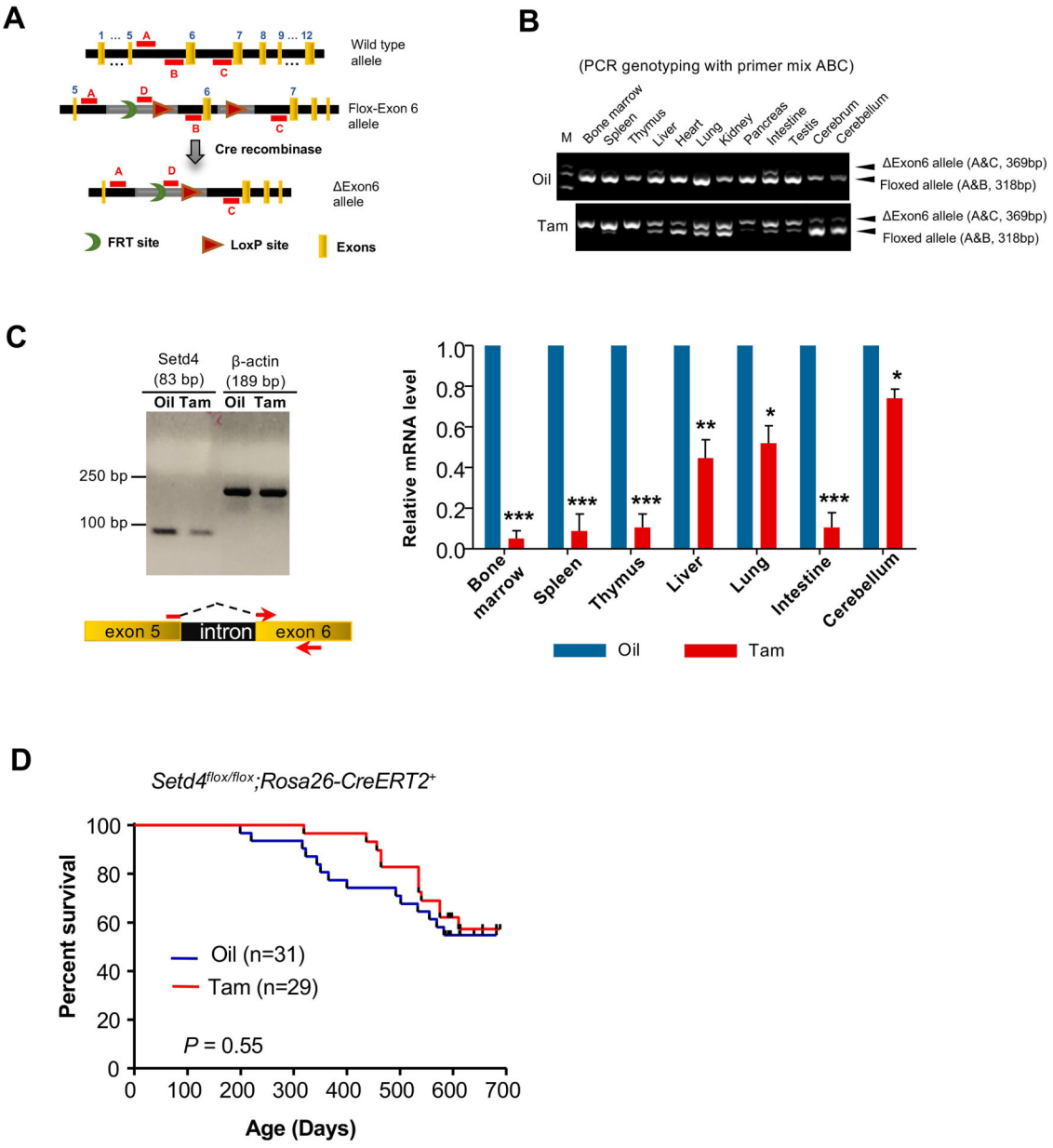

Fig. 1. Verification of tamoxifen (Tam) -induced deletion of Setd4 exon- 6 in mice.

(A) The genomic DNA configuration of the three Setd4 alleles. Exon 6 of the wild type allele was flanked by two LoxP sites inserted into introns 5 and 6 to produce the floxed Setd4 allele. Upon Cre-mediated recombination between the LoxP sites, exon 6 is excised to produce the ΔExon6 allele. The locations of primers used for PCR based genotyping and the expected product size are indicated as red lines above (forward primers) or below (reverse primers) each allele and are labeled A-D. See Table S3 for the expected sizes of PCR products using the indicated primer pairs.

(B) Multiplex PCR assay demonstrating Setd4 exon 6 deletion. PCR analysis of DNA from the indicated tissues for a representative pair of *Setd4*$^{flox/flox}$*;Rosa26-CreERT2*$^{+}$ littermates mice that were injected with Tam or with oil as a negative control (Oil) are shown. The

primers A, B, and C (as shown in panel A) were used for the PCRs. The upper band corresponds to the ΔExon6 allele (369 bp, primers A and C), and the lower band is the resulting PCR product from floxed allele (318 bp, primers A and B). Tam treatment converted the majority of floxed allele to the ΔExon6 allele in most of the tissues, except for the cerebrum and cerebellum, likely due to restricted entry of Tam through the blood-brain-barrier.

(C) qRT-PCR verification of Setd4 mRNA downregulation in Tam-treated mice. A primer overlapping the junction between exons 5 and 6 was used for to assay for Setd4 mRNA down regulation by qRT-PCR from the indicated tissues. The primer locations are indicated by red arrows. The correct product size at PCR completion was verified for both Setd4 and β-actin cDNA by agarose electrophoresis (left). The bar graph (right) represents the Setd4 mRNA levels relative β-actin levels for the indicated tissues. Error bars represent SDs of the means, based on the results of three independent repeats.

(D) Kaplan-Meier survival curves of Tam and Oil treated *Setd4*$^{flox/flox}$*;Rosa26-CreERT2*$^{+}$ mice. Six-to-eight week-old mice were injected with Tam or Oil (as control) 5 daily times. A total of 31 Oil and 29 Tam treated *Setd4*$^{flox/flox}$*;Rosa26-CreERT*$^{+}$ mice were monitored for up to 700 days of age. $p = 0.55$ (log-rank Mantel–Cox test).

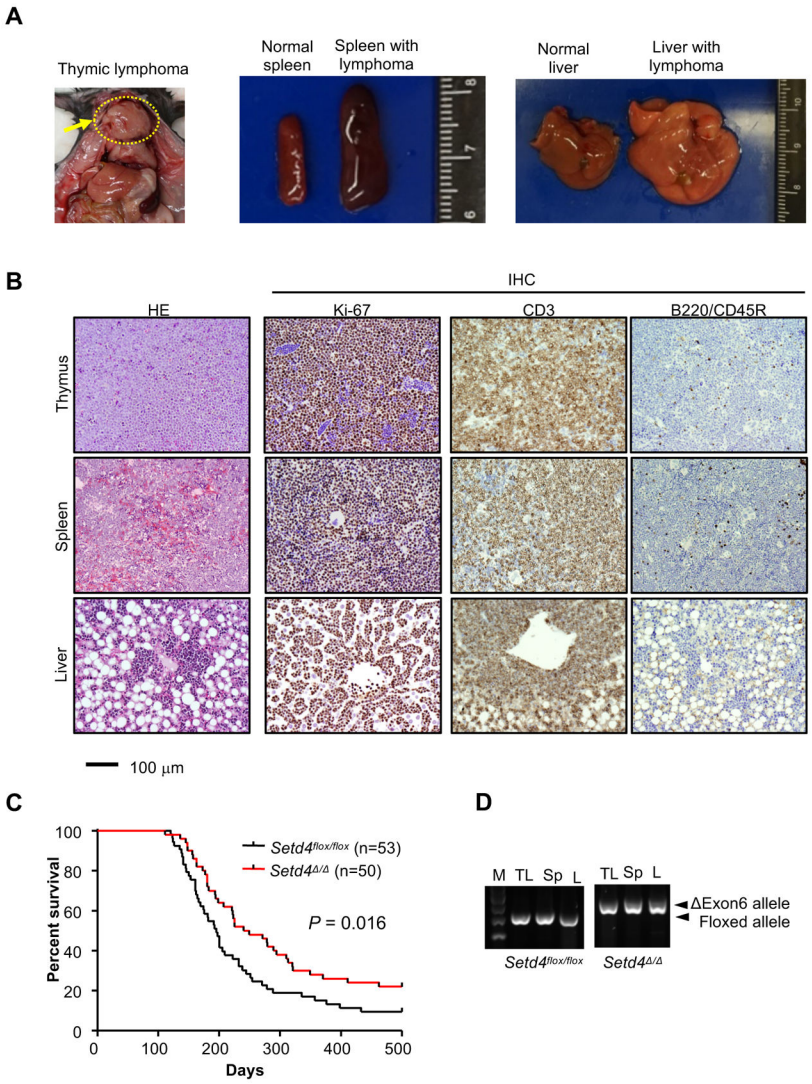

Fig. 2. Loss of *Setd4* extends the survival from radiation-induced T-lymphoma.

Sex matched littermates of *Setd4*$^{flox/flox}$;*Rosa26-CreERT2*$^{+}$ were treated with tamoxifen or oil to produce *Setd4*$^{\Delta/\Delta}$ or and *Setd4*$^{flox/flox}$ mice. These mice were exposed to four weekly 2 Gy of γ-irradiation (4×2Gy), and the long-term survival were monitored for 500 days after irradiation.

(A) Representative gross features of thymic lymphoma. Note the mouse usually carried a large thymic lymphoma and enlarged spleen or liver.

(B) H&E and immunohistochemistry (IHC) staining of representative tumors. The tumor cells in thymus and infiltrated organs (spleen and liver) were stained for Ki-67, CD3 and B220/CD45R. Magnification: 100x. Scale Bar: 100 μM.

(C) Kaplan-Meier survival of sex-matched littermate *Setd4*$^{\Delta/\Delta}$ (n=50) and *Setd4*$^{flox/flox}$ (n=53) mice. Shown are the days of survival since the beginning of irradiation. The median survival was 245 days for *Setd4*$^{\Delta/\Delta}$, and 195 days for *Setd4*$^{flox/flox}$. P = 0.016 (log-rank Mantel–Cox test).

(D) Representative genotypes of tumor DNA obtained from thymic lymphoma (TL), Spleen (Sp), and livers (L) using multiplex PCR that simultaneously detect the wt, Flox-Exon6, and ΔExon6 alleles.

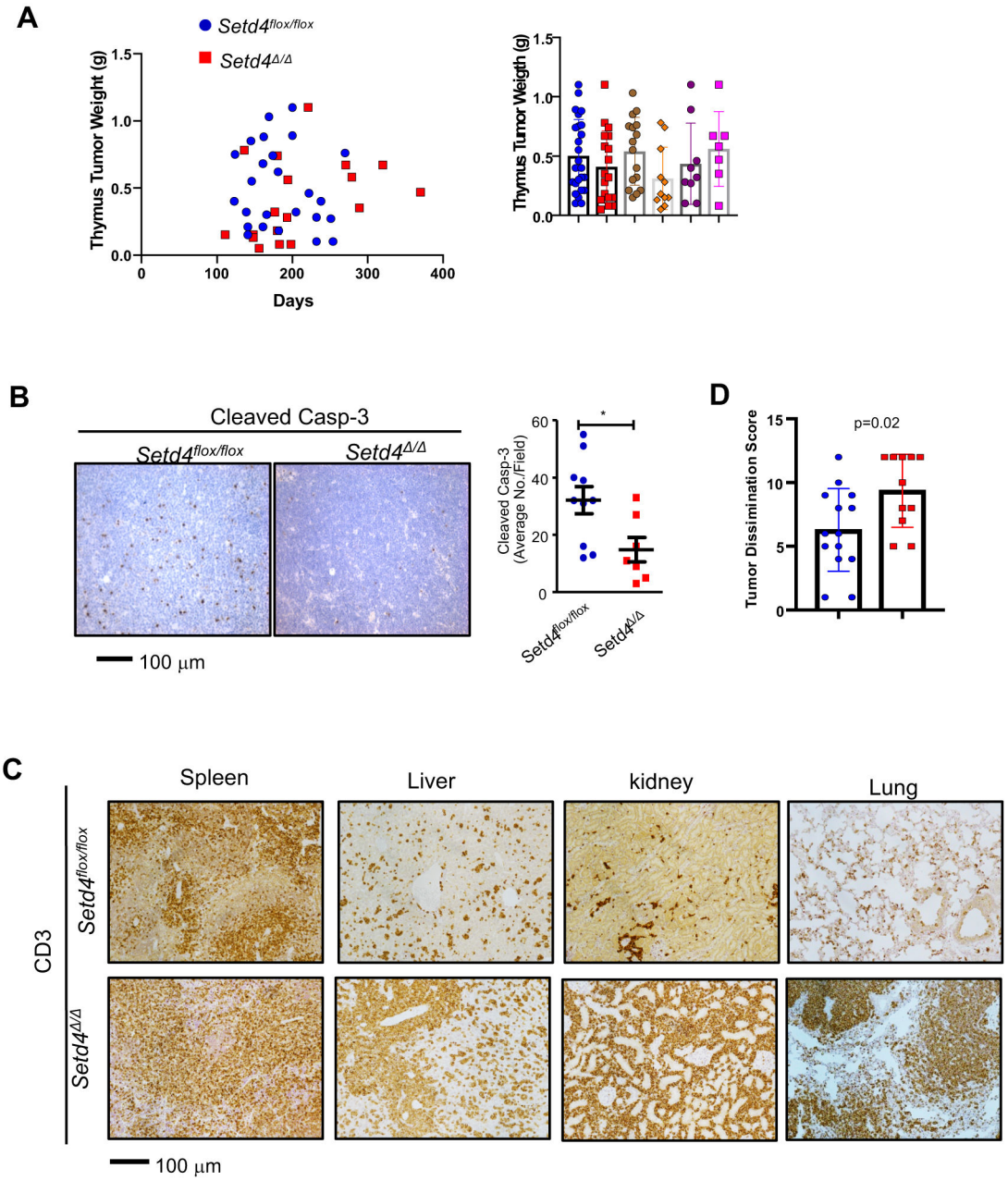

Fig. 3. Characterizations of tumor size and dissemination.

(A) Left panel: Plot of thymic lymphoma tumor weight on the day of death. Right panel: comparison of tumor weight between *Setd4*$^{\Delta/\Delta}$ and *Setd4*$^{flox/flox}$ mice. P=0.32 (all cases), p=0.046 (cases died within 195 days), p=0.47 (case died after 195 days).

(B) Representative IHC staining (left) of cleaved caspase-3 and quantitative comparison (right).

(C) Representative IHC staining of CD3 in peripheral organs, including spleen, liver, kidney, and lung.

(D) Tumor dissemination score based on a semi-quantitative estimation of tumor infiltration in spleen, liver, kidney, and lung (Table 1). p =0.02.

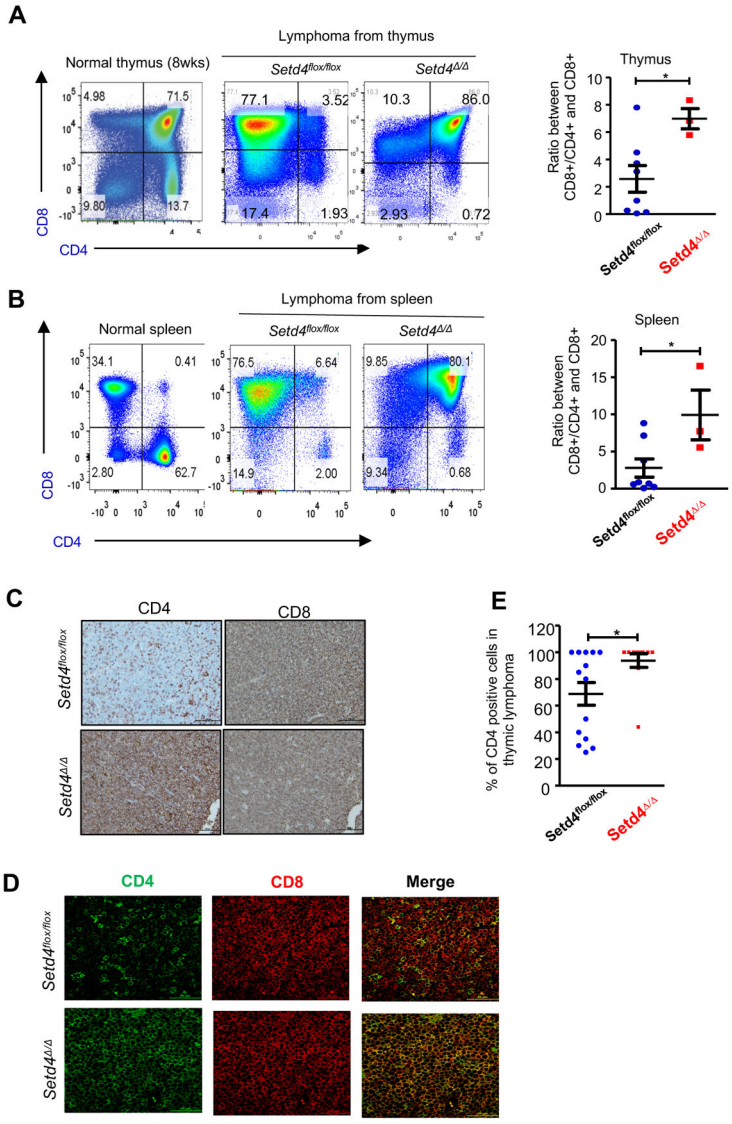

Fig. 4. Different subtypes of thymic lymphoma in *Setd4*$^{\Delta/\Delta}$ and *Setd4*$^{flox/flox}$ mice.

(A, B) Cell suspension of fresh thymic lymphoma tissues and spleen were used to stain for the CD4 and CD8 markers and analyzed by flow cytometer. (A) shows a set of representative flow cytometric profiles in a normal thymus, and thymic tumor cells of *Setd4*$^{\Delta/\Delta}$ and *Setd4*$^{flox/flox}$ mice. (B) shows representative flow cytometric profiles in a normal spleen and tumor infiltrated spleens of *Setd4*$^{\Delta/\Delta}$ and *Setd4*$^{flox/flox}$ mice. Right panels show the ratios between $CD8^+/CD4^+$ double positive cells and $CD8^+/CD4^-$ cells. *: $p < 0.05$ based on unpaired Student t test.

(C) Representative IHC staining of CD4 and CD8 of thymic lymphoma. Scale bar: 100 μm.

(D) Representative fluorescent-IHC staining of CD4 and CD8 of thymic lymphoma. Scale bar: 50 μm.

(E) Percentage of CD4 and CD8 positive cells in thymic lymphoma as identified by IHC and fluorescent-IHC. *Setd4*$^{flox/flox}$ (n=14), *Setd4*$^{\Delta/\Delta}$ (n=11)

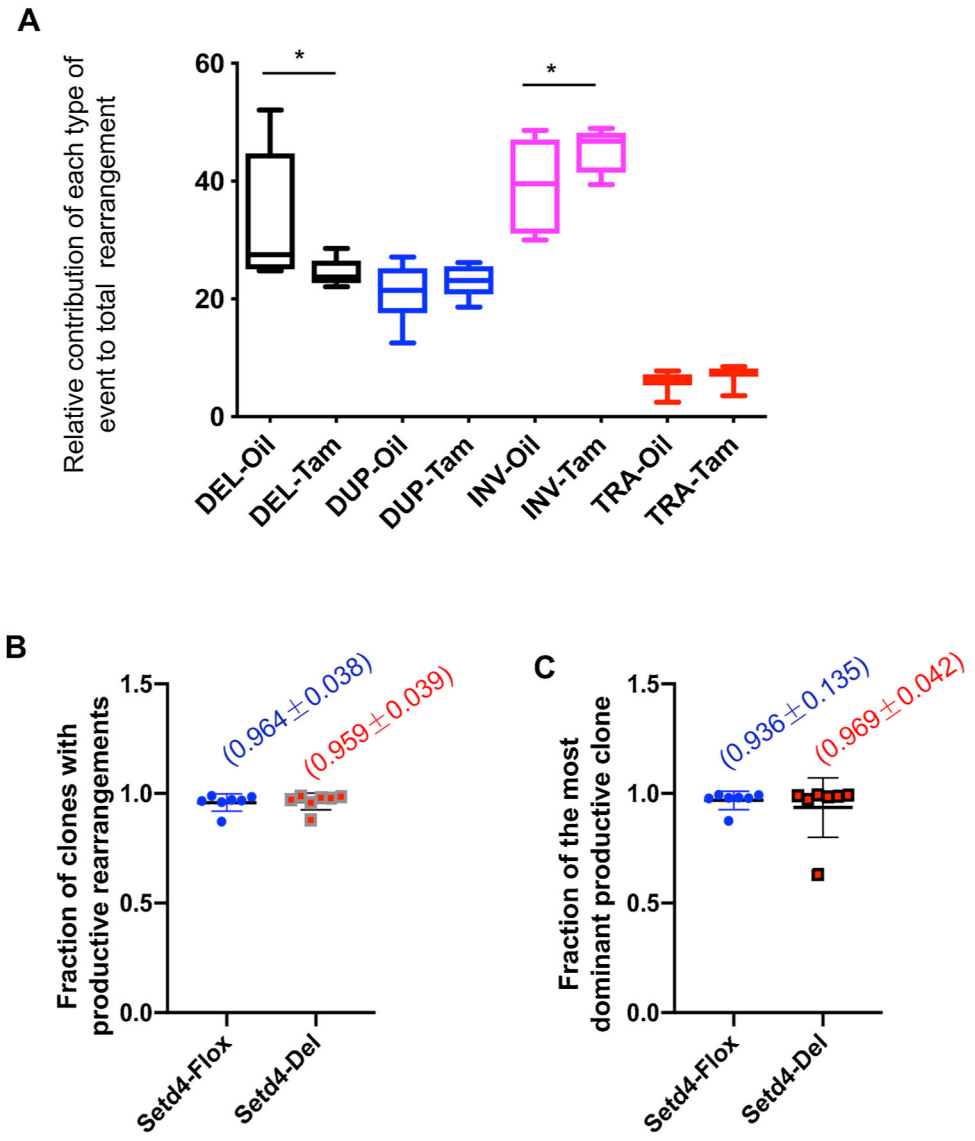

Fig. 5. Genomic rearrangements and clonality in radiation-induced T-lymphomas.

(A) Proportional burden of deletion (DEL), duplication (DUP), inversion (INV), and translocation (TRA) events in the lymphoma genomes in *Setd4*$^{\Delta/\Delta}$ (Tam) and *Setd4*$^{flox/flox}$ (Oil) mice. *: $p < 0.05$.

(B) The factions of lymphoma cells containing productive TCR recombination.

(C) The fractions of the most dominant clone among the lymphoma cells with productive TCR recombination.

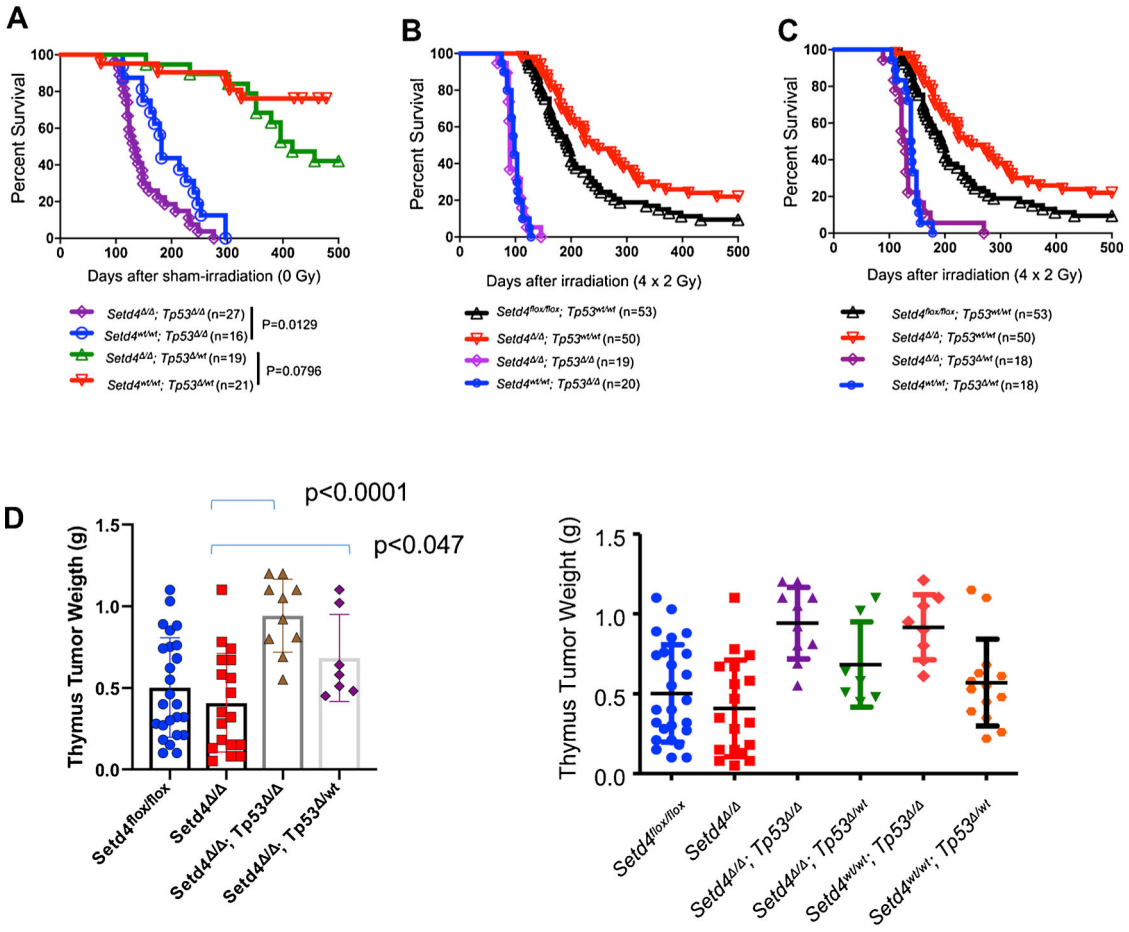

Fig. 6. Effects of *Setd4* deficiency on radiation-induced T-lymphoma in Tp53 deficient mice.

(A) Effects of *Setd4* deletion on spontaneous tumor formation in $Tp53^{\Delta/\Delta}$ and $Tp53^{\Delta/wt}$ mice. Adult mice (8-10 weeks) of $Setd4^{flox/flox};Tp53^{flox/flox};Rosa26\text{-}CerERT2^{+}$ ($Setd4^{\Delta/\Delta};Tp53^{\Delta/\Delta}$, n=27), $Setd4^{wt/wt};Tp53^{flox/flox};Rosa26\text{-}CerERT2^{+}$ ($Setd4^{wt/wt};Tp53^{\Delta/\Delta}$, n=16), $Setd4^{flox/flox};Tp53^{flox/wt};Rosa26\text{-}CerERT2$ ($Setd4^{\Delta/\Delta};Tp53^{\Delta/wt}$, n=19), and $Setd4^{wt/wt};Tp53^{flox/wt};Rosa26\text{-}CerERT2^{+}$ ($Setd4^{wt/wt};Tp53^{\Delta/wt}$, n=21) were treated with tamoxifen to induce *Tp53* and/or *Setd4* deletion, and the spontaneous tumor formation were monitored and presented. Values of log-rank Mantel–Cox tests are: $Setd4^{wt/wt};Tp53^{\Delta/\Delta}$ vs. $Setd4^{\Delta/\Delta};Tp53^{\Delta/\Delta}$, p = 0.013; $Setd4^{wt/wt};Tp53^{\Delta/wt}$ vs $Setd4^{\Delta/\Delta};Tp53^{\Delta/wt}$, p = 0.08.

(B) Effect of *Setd4* deletion on radiation-induced tumorigenesis in homozygous $Tp53^{\Delta/\Delta}$ mice. Adults $Setd4^{wt/wt};Tp53^{flox/flox}$;Rosa26-CreERT2^{+} ($Setd4^{wt/wt};Tp53^{\Delta/\Delta}$, n=20), and $Setd4^{flox/flox};Tp53^{flox/flox}$;Rosa26-CreERT2^{+} ($Setd4^{\Delta/\Delta};Tp53^{\Delta/\Delta}$, n=19) were treated with tamoxifen, irradiated, and monitored for tumor formation. The same survival curves of $Setd4^{flox/flox};Tp53^{wt/wt}$ (n=53) and $Setd4^{\Delta/\Delta};Tp53^{wt/wt}$ (n=50) as in Fig. 2C are re-plotted here for the purpose of comparison.

(C) Effect of Setd4 deletion on radiation induced tumorigenesis in heterozygous $Tp53^{\Delta/wt}$ mice. Adults Rosa26-CreERT2 positive $Setd4^{wt/wt};Tp53^{flox/wt}$;Rosa26-CreERT2^{+} ($Setd4^{wt/wt};Tp53^{\Delta/wt}$, n=18), and $Setd4^{flox/flox};Tp53^{flox/wt}$;Rosa26-CreERT2^{+} ($Setd4^{\Delta/\Delta};Tp53^{\Delta/wt}$, n=18) were treated with tamoxifen, irradiated, and monitored for tumor

formation. The same survival curves of *Setd4*$^{flox/flox}$;*Tp53*$^{wt/wt}$ (n=53) and *Setd4*$^{\Delta/\Delta}$;*Tp53*$^{wt/wt}$ (n=50) as in Fig. 2C are re-plotted here for the purpose of comparison. (D) Weight of radiation-induced thymus tumors at the time of animal death in *Setd4* and *Tp53* deficient mice.

Table 1.

Infiltration of thymic lymphoma in peripheral organs

Genotype	Case ID	Survival days post TBI	Degree of tumor infiltration			
			Spleen	Liver	Kidney	Lung
Setd4$^{flox/flox}$	1825	181	++	++	–	–
	1826	169	++	+	–	+
	1827	138	–	–	–	+
	1828	182	++	+++	++	++
	1829	166	++	++	+	+
	919-1	124	+	+++	–	+
	927-1	141	+	+++	+++	++
	927-2	141	+++	+++	+	+++
	1001-1	145	++	+	+	+
	1026-1	161	+	+++	+	+
	1108	174	+++	+++	+++	+++
	1204-1	200	+	+	+++	+++
	1204-2	200	++	+++	++	+
	1830	270	+	–	–	–
	1831	278	+++	+++	++	–
Setd4$^{\Delta/\Delta}$	1818	289	+++	+++	+++	+++
	1819	279	+++	+++	+++	+++
	1216	221	++	+++	++	+++
	1821	161	+++	+++	+++	+++
	1822	180	++	+	++	++
	1823	177	+	++	+	++
	1824	148	+++	++	++	+
	913/906	111	+++	+++	+++	+++
	1001-2	135	+	+	+	++
	1127	193	+++	+++	+++	+++

The scores were based on IHC staining of CD3.

-: <5% of cells are T-cell marker positive.

+: 5-30% of cells are T-cell marker positive.

++: 30-60% of cells are T-cell marker positive.

+++: >60% of cells are T-cell marker positive.